

Vortex motion in magnetic disks with different geometric asymmetry

Kuo-Ming Wu, Jia-Feng Wang, Yin-Hao Wu, Ching-Ming Lee, Jong-Ching Wu, and Lance Horng

Citation: *Journal of Applied Physics* **103**, 07F314 (2008); doi: 10.1063/1.2834251

View online: <http://dx.doi.org/10.1063/1.2834251>

View Table of Contents: <http://scitation.aip.org/content/aip/journal/jap/103/7?ver=pdfcov>

Published by the [AIP Publishing](#)

Articles you may be interested in

[Vortex annihilation in magnetic disks with different degrees of asymmetry](#)

J. Appl. Phys. **113**, 103905 (2013); 10.1063/1.4795115

[Anomalous, hysteretic, transverse magnetoresistance in superconducting thin films with magnetic vortex arrays](#)

Appl. Phys. Lett. **94**, 252507 (2009); 10.1063/1.3159466

[Vortex motion in chirality-controlled pair of magnetic disks](#)

Appl. Phys. Lett. **90**, 132501 (2007); 10.1063/1.2716861

[Noninvasive magnetic imaging and magnetization measurement of isolated mesoscopic Co rings](#)

Appl. Phys. Lett. **81**, 3413 (2002); 10.1063/1.1518564

[Dynamic scaling of magnetic hysteresis in micron-sized Ni 80 Fe 20 disks](#)

Appl. Phys. Lett. **74**, 1609 (1999); 10.1063/1.123632

 **SHIMADZU**
Excellence in Science

Powerful, Multi-functional UV-Vis-NIR and FTIR Spectrophotometers

Providing the utmost in sensitivity, accuracy and resolution for applications in materials characterization and nano research

- Photovoltaics
- Polymers
- Thin films
- Paints
- Ceramics
- DNA film structures
- Coatings
- Packaging materials

[Click here to learn more](#)

A row of four Shimadzu spectrophotometers is shown. From left to right: a small benchtop model, a larger benchtop model with a sample holder, a large floor-standing model with a wide entrance, and a tall, narrow floor-standing model.

Vortex motion in magnetic disks with different geometric asymmetry

Kuo-Ming Wu,¹ Jia-Feng Wang,¹ Yin-Hao Wu,² Ching-Ming Lee,³ Jong-Ching Wu,¹ and Lance Horng^{1,a)}

¹Department of Physics and Taiwan SPIN Research Center, National Changhua University of Education, Changhua 50007, Taiwan

²Graduate Institute of Photonics, National Changhua University of Education, Changhua 50007, Taiwan

³General Education Center and Taiwan SPIN Research Center, National Yunlin University of Science and Technology, Yunlin 64002, Taiwan

(Presented on 6 November 2007; received 12 September 2007; accepted 29 October 2007; published online 19 February 2008)

An asymmetric disk achieves control over the clockwise and counterclockwise vortex states in a magnetic disk with an in-plane magnetic field. In this study, the influence of different geometric asymmetry on the vortex motion in 800 nm disks has been studied. The excised angle, defined as half of the center angle corresponding to the excised arc, is flattened varying from 15° to 90° . For each asymmetric degree disk, the vortex motion is investigated through anisotropic magnetoresistance measurement and hysteresis loops recorded by focused magneto-optic Kerr effect magnetometry. The vortex nucleation and annihilation fields show strong dependence and different sensitivity on the asymmetry of disk. An interestingly evident switching mode change is also observed at particular excised angle. Numerical simulations, corresponding to realistically identical system, are calculated and agree well with the experimental results. © 2008 American Institute of Physics.

[DOI: [10.1063/1.2834251](https://doi.org/10.1063/1.2834251)]

I. INTRODUCTION

One of the challenges in the development of high density digital data storage media and magnetoresistance memory chips is reducing the interaction between adjacent magnetic elements. It is well known that a single domain magnetic element introduces a distribution of stray field which may lead to unrepeatable switching of other bits.¹ Vortex structures that stabilize in ferromagnetic dots^{2–4} and rings^{5,6} have high potential as unit element for high density magnetic storage because of the negligible magnetostatic interaction. Compared to single domain states, magnetic vortices have a much lower stray field due to the closure magnetic flux configuration and, thus, can be more closely packed. Previous studies have shown that circular-patterned magnetic dots in vortex state, the vortex core arises a shift motion perpendicular to the direction of external field.^{3,7,8} The magnetization rotation can be statistically separated into clockwise (CW) and counterclockwise (CCW) vortices. However, the appearance of CW or CCW vortex could not be controlled on purpose by applying an in-plane magnetic field⁹ because the in-plane shape anisotropic energy is isotropic. In the past few years, some efforts have been made on asymmetric disks to achieve the control over the CW/CCW vortex states in magnetic disks with an in-plane magnetic field.^{10–12}

Besides the technological application, magnetic vortices in patterned magnetic elements are of interest also from a physics point of view. The vortex nucleation and annihilation mechanism have been investigated for symmetric and asymmetric dots, both experimentally and theoretically.^{2,8–10,12–14}

However, not many investigations report how this mechanism is altered in the case of disks with different geometric asymmetry.

In this study, we exhibit a new aspect, controlling the vortex motion by the size of cut of the disk. Experimental observations by anisotropic magnetoresistance (AMR) electric measurement and focused magneto-optic Kerr effect (FMOKE), together with numerical micromagnetic simulations, have shown the nucleation and annihilation fields of vortex to have strong correlation with the asymmetry of excised magnetic disks.

EXPERIMENT

Circular $\text{Ni}_{80}\text{Fe}_{20}$ (Permalloy, Py) disks with 800 nm diameter, 40 nm thick, and excised angles varying from 15° to 90° were fabricated by electron beam lithography and lift-off technique, where the excised angle (θ) indicates half central angle corresponding to the excised arc, as shown in Fig. 1(a). Figures 1(b)–1(d) display the scanning electron microscopy

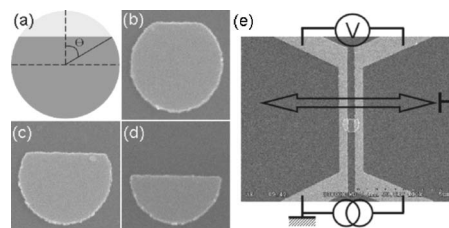


FIG. 1. (a) Schematic illustration of defining excised angle that is corresponding to half central angle of the excised arc. [(b)–(d)] SEM images of 800 nm asymmetric Py disks with θ of 30° , 60° , and 90° , respectively. (e) SEM image of $\theta=60^\circ$ Py disk connected with electrical bridge for four-point probe measurement. The cartoons illustrate the meter installation and the two head arrow represents the direction of external magnetic field.

a)Electronic mail: phlhorng@cc.ncue.edu.tw.

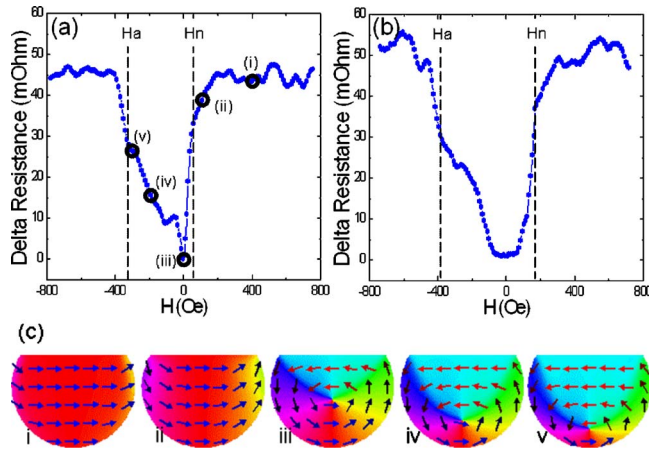


FIG. 2. (Color online) Delta resistance of $\theta=$ (a) 60° , (b) 45° Py disk as a function of the in-plane horizontal magnetic field. The magnetic field is swept from +800 to -800 Oe. (c) Corresponding simulated magnetization distributions for $\theta=60^\circ$ Py disk at different external fields: (i) saturation state in positive field of 400 Oe, (ii) C state at 100 Oe, which below saturation field and before vortex nucleating, (iii) vortex state in zero magnetic fields, (iv) a shift motion of vortex core perpendicular to the field direction at -200 Oe, and (v) vortex state at -300 Oe, before annihilation.

(SEM) images of prepared disks with excised angles of 30° , 60° , and 90° , respectively. Ta (100 nm)/Au (50 nm) bridge circuit is connected to each disk for R - H measurement and the illustration for traditional four-point probe electric property measurement is shown in Fig. 1(e). On the other hand, the Py dots with the same excised angle are arranged in $100 \times 100 \mu\text{m}^2$ area and disposed in a square lattice for FMOKE magnetometry. For dots, the interdot separation, defined as the distance between the dot centers, is 1600 nm and the excised angle is varied yielding arrays with θ of 15° , 30° , 45° , 60° , 75° , and 90° . The anisotropic magnetoresistance versus external field (R - H) loops and the FMOKE hysteresis loops, recorded with laser beam of 632.8 nm wavelength and $50 \mu\text{m}$ spot in longitudinal geometry, were carried out at room temperature with external magnetic field applying parallel to the flat edge. Note that the FMOKE hysteresis loop represents a superposition of the identically constituent elements in the array. Namely, all the magnetic interactions in array will be recorded.

Micromagnetic simulations of domain structure in 800 nm asymmetric Py disks were calculated by object oriented micromagnetic framework (OOMMF) software.¹⁴ Here, the cell size, the saturation magnetization M_s , the exchange constant, and the damping parameter are 5 nm, $700 \times 10^3 \text{ A/m}$, $10 \times 10^{-12} \text{ J/m}$, and 0.5, respectively.

III. RESULTS AND DISCUSSION

Figures 2(a) and 2(b) depict the relationship between the resistance changes with the in-plane applied field, measured by traditional dc four-probe method. Here, the dc flowing in the disk is fixed at $20.000 \mu\text{A}$ and the element voltage is measured using a high sensitivity nano-voltage meter ($\sim 10 \text{ nV}$). With external field sweeping from +800 to -800 Oe, the delta resistance $[R(H) - R(0)]$ due to AMR is clearly observed with two jumps corresponding to the field of vortex nucleation (H_n) and annihilation (H_a) for the Py

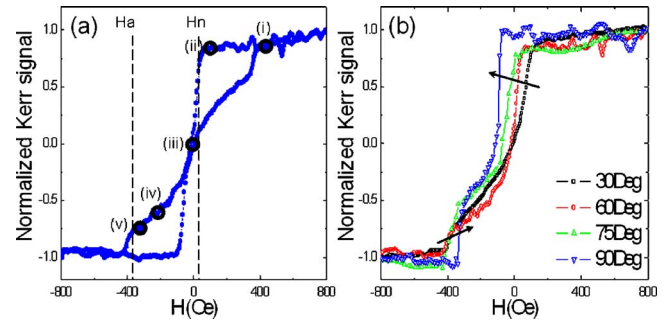


FIG. 3. (Color online) (a) Longitudinal MOKE hysteresis loop of $\theta=60^\circ$ Py disk array. The corresponding magnetic structures (i)–(v) are homologous with Fig. 2(c). (b) Half hysteresis loops of $\theta=30^\circ$, 60° , 75° , 90° Py disk arrays. The magnetic field, similar to R - H measurement, is swept from +800 to -800 Oe.

disk with $\theta=60^\circ$ at 59.3 and -331 Oe, respectively. Figures 2(c)(i)–2(c)(v) show the domain structures calculated by micromagnetic simulations at external fields of 400, 100, 0, -200, and -300 Oe, respectively. For large positive value of external field, the disk is in a saturation state (or single domain state, SD state) configuration [Fig. 2(c)(i)] and corresponds to the high resistance state since almost all moments are parallel to current direction [Fig. 2(a)(i)]. Starting from the SD configuration and decreasing the field, the resistance value gradually reduces [Fig. 2(a)(ii)] before the field H_n as a result of the magnetic structure transiting from the SD state to the C state [Fig. 2(c)(ii)]. By further decreasing the field, the vortex nucleates from the flat edge at field H_n and causes a sudden drop on resistance, and then the core moves toward the disk center. The vortex nucleates from the flat edge where the demagnetizing field is larger than that at the round edge.^{8,12} When the vortex core slides to the geometric center of disk (not the original center of circle) [Fig. 2(c)(iii)] to closure the magnetic flux at zero fields, the resistance comes to a minimum value [Fig. 2(a)(iii)]. Upon zero field and then increasing the field in the opposite direction, the vortex moves from the geometric center toward the round edge [Figs. 2(c)(iv) and 2(c)(v)] that leads the resistance to a gentle increase [Fig. 2(a)(iv) and 2(c)(v)]. Finally, above the H_a , the vortex is expelled from the disk and the magnetic structure becomes a reverse C state, and then achieves a reverse SD state again. To observe the influence of different asymmetry on vortex motion, compared with $\theta=60^\circ$ Py disk, Py disk with $\theta=45^\circ$ has evidently larger H_n and H_a of 153 and -384 Oe, respectively, as shown Fig. 2(b). As θ decreases, the proportion of curve edge to flat edge increases and the anisotropy axis becomes unapparent so that a vortex type magnetic structure results in a lower magnetostatic energy and anisotropy energy. Namely, the disk with smaller θ prefers to stay at vortex state, which induces the variation of H_n and H_a in Figs. 2(a) and 2(b).

To investigate vortex motion from the view of net magnetization, the FMOKE hysteresis loop, recorded for an array of Py disks with $\theta=60^\circ$, is shown in Fig. 3(a). The hysteresis loop also exhibits two obviously drops corresponding to vortex nucleation and annihilation at field values of 40.4 and -360 Oe, respectively. Concerning the comparison with previous AMR measurement, the reason that the fields H_n and

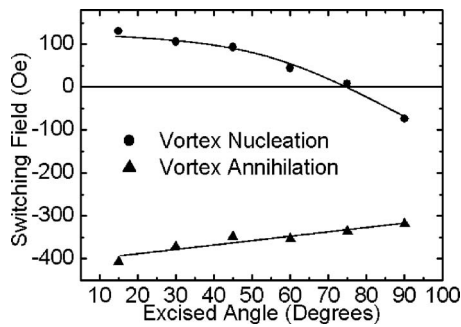


FIG. 4. Analyzed vortex nucleation and annihilation fields as a function of excised angle for 800 nm Py disk arrays. The solid guide lines show the trends of H_n and H_a .

H_a , analyzed from R - H loops and hysteresis loops, are slightly different is that probably it is a consequence of the relatively weak interactions between elements in the disk array.⁸ As mentioned above, the simulated magnetic structures in Fig. 2(c) can be related to the positions of (i)–(v) in this hysteresis [Fig. 3(a)] loop that represents a contrast between electric and magnetic properties for $\theta=60^\circ$ Py disk. We stress that the magnetization goes to almost zero value in zero external fields at the (iii) position of Fig. 3(a), which proves that the vortex core stays at the geometric center instead at the original center of the disk and forms a closed magnetic flux, resulting in a zero net magnetization. Figure 3(b) displays the hysteresis loops of disk arrays with $\theta=30^\circ$, 60° , 75° , and 90° dots. As the excised angle θ increases, a negative shift of H_n field and a positive shift of H_a field are evidently presented. If examined carefully, the loops for θ smaller than 60° are crossing at the zero point but not for θ larger than 75° . Interestingly, the 800 nm Py disk with small excised angle ($\geq 60^\circ$) expresses a circle-pattern-like switching process, in which magnetic moments tend to form vortex structure and zero net magnetization at zero external field.^{8,15} The Py disk with larger excised angle ($\leq 75^\circ$), higher aspect ratio, implies an ellipse-(or rectangle-) pattern-like reversal behavior that magnetic moments prefer to stay at saturation state under zero external fields due to the higher effective anisotropy axis.^{16,17} Here, we would like to define that the saturation state is as a state where the magnetic moments are aligned approximately parallel, and small departures of angle from the means of total magnetization direction are acceptable. Finally, the H_n and H_a of asymmetric disk with different θ , analyzed from MOKE hysteresis loops, are plotted in Fig. 4 and the solid guide lines show the trends of H_n and H_a . The fields of vortex nucleation are more sensitive to the excised angle than the field of vortex annihilation. It is found that the magnetization switching behavior changes from circle-pattern-like mode to ellipse-pattern-like mode at the excised angle around 75° in 800 nm asymmetric Py disk. This could be considered that the effect of aniso-

tropy energy is rather small and, therefore, can be ignored for small θ disk and become more important with θ increasing. Py disk with θ higher than 75° presents a saturation state at zero external fields and a vortex state at negative field, since the curve edge in disk is still much longer than the flat edge, a preferred vortex structure would still be induced by the curved edge.

IV. CONCLUSION

We have studied the vortex motion in asymmetric Py disk with various excised angles from the views of electric property, net magnetization, and numerical simulation. The results are consistent well with each other. It is found that the nucleation and annihilation fields depend on the excised angle, and the nucleation field is more sensitive to excised angle than the annihilation field. The magnetization switching mode changes at the excised angle around 75° in 800 nm Py disk. The variation of anisotropy energy, changed by geometric asymmetry influence, reflected both in the vortex nucleation and annihilation, shows a way of controlling the switching field and switching mode of patterned magnetic device on purpose.

ACKNOWLEDGMENTS

This work was supported by Ministry of Economic Affairs, Taiwan, under Grant No. 96-EC-17-A-01-S1-026.

- ¹T. Aign, P. Meyer, S. Lemerle, J. P. Jamet, J. Ferre, V. Mathet, C. Chappert, J. Gierak, C. Vieu, F. Rousseaux, H. Launois, and H. Bernas, *Phys. Rev. Lett.* **81**, 5656 (1998).
- ²R. P. Cowburn, D. K. Koltsov, A. O. Adeyeye, M. E. Welland, and D. M. Tricker, *Phys. Rev. Lett.* **83**, 1042 (1999).
- ³T. Shinjo, T. Okuno, R. Hassdorf, K. Shigeto, and T. Ono, *Science* **289**, 930 (2000).
- ⁴Y. H. Hoffmann and F. Steinbauer, *J. Appl. Phys.* **92**, 5463 (2002).
- ⁵S. P. Li, D. Peyrade, M. Natali, A. Lebib, Y. Chen, U. Ebels, L. D. Buda, and K. Ounadjela, *Phys. Rev. Lett.* **86**, 1102 (2001).
- ⁶K. Bussmann, G. A. Prinz, R. Brass, and J. G. Zhu, *Appl. Phys. Lett.* **78**, 2029 (2001).
- ⁷J. Raabe, R. Pulwey, R. Sattler, T. Schweinbock, J. Zweck, and D. Weiss, *J. Appl. Phys.* **88**, 4437 (2000).
- ⁸M. Natali, I. L. Prejbeanu, A. Lebib, L. D. Buda, K. Ounadjela, and Y. Chen, *Phys. Rev. Lett.* **88**, 157203 (2002).
- ⁹M. Schneider, H. Hoffmann, and J. Zweck, *Appl. Phys. Lett.* **77**, 2909 (2000).
- ¹⁰M. Schneider, H. Hoffmann, and J. Zweck, *Appl. Phys. Lett.* **79**, 3113 (2001).
- ¹¹R. Nakatani *et al.*, *J. Magn. Magn. Mater.* **286**, 31 (2005).
- ¹²T. Kimura, Y. Otani, H. Masaki, T. Ishida, R. Antos, and J. Shibata, *Appl. Phys. Lett.* **90**, 132501 (2007).
- ¹³A. Fernandez and C. J. Cerjan, *J. Appl. Phys.* **87**, 1395 (2000).
- ¹⁴<http://math.nist.gov/oommf/>
- ¹⁵K. Yu. Guslienko, V. Novosad, Y. Otani, H. Shima, and K. Fukamichi, *Phys. Rev. B* **65**, 024414 (2001).
- ¹⁶L. M. Malkinski, M. Yu, A. Y. Vovk, D. J. Scherer II, L. Spinu, W. Zhou, S. Whittenburg, Z. Davis, and J. S. Jung, *J. Appl. Phys.* **101**, 09J110 (2007).
- ¹⁷E. Girgis, J. Schelten, J. Shi, J. Janesky, S. Tehrani, and H. Goronkin, *Appl. Phys. Lett.* **76**, 3780 (2000).